

**Electronic Supplementary Information (ESI) for**

**Narrow Response Temperature Range with Excellent  
Reversible Shape Memory Effect for Semi-Crystalline  
Networks as Soft Actuators**

Dequan Chi,<sup>a</sup> Haoyu Gu,<sup>a</sup> Jingfeng Wang,<sup>c</sup> Chao Wu,<sup>a</sup> Ruijie Wang,<sup>a</sup> Zhongjun  
Cheng,<sup>a</sup> Dongjie Zhang,<sup>a</sup> Zhimin Xie,<sup>b</sup> and Yuyan Liu,<sup>a,\*</sup>

<sup>a</sup>MIIT Key Laboratory of Critical Materials Technology for New Energy Conversion and Storage,  
School of Chemistry and Chemical Engineering, Harbin Institute of Technology, Harbin 150001,  
P. R. China

<sup>b</sup>National Key Laboratory of Science and Technology on Advanced Composites in Special  
Environments, Harbin Institute of Technology, Harbin 150080, P. R. China

<sup>c</sup>Northwest Institute for Nonferrous Metal Research, Xi'an 710016, China.

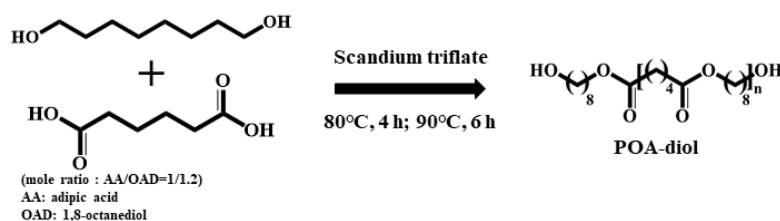
\* Lead contact, Corresponding author

E-mail addresses: liuyy@hit.edu.cn

## 1. Experimental Section

### 1.1 Synthesis of poly(octylene adipate)-diol (POA-diol)

POA-diol was synthesized via a two-stage melt polymerization including esterification and melt polycondensation. The synthesis process was follows: both (15.0 g, 0.103 mol) adipic acid and 1, 8-octanediol (17.7 g, 0.121 mol) were added to a three-neck flask. Then, they were heated to 80°C with stirring under a nitrogen atmosphere until completely melted. Scandium triflate (0.15 g) was added to the flask as a catalyst. Immediately, the whole system was stirred at 80°C for 4 h. Afterwards, the system was heated to 90°C and continued to react for 6 h under vacuum conditions (vacuum level of about 20 Pa). The crude product was dissolved in a minimum volume of CHCl<sub>2</sub>, precipitated into excess petroleum ether, and then recovered by filtration and drying under reduced pressure to constant weight.

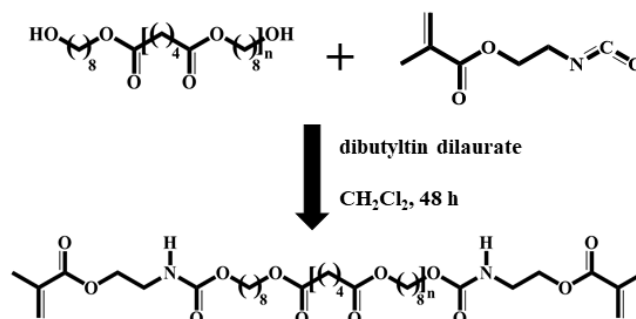


Scheme 1. Synthesis of POA-diol.

### 1.2 Synthesis of POA-dimethacrylate (POA-DA)

POA-diol (5 g,  $0.7 \times 10^{-3}$  mol) was added to a single-mouth flask. Then, 25 mL of dichloromethane was added to the flask. After POA-diol was completely dissolved, 2,2-isocyanatoethyl methacrylate (0.28 g,  $1.8 \times 10^{-3}$  mol) and dibutyltin dilaurate (0.1 mL) were added, where dibutyltin dilaurate served as a catalyst. Subsequently, the flask was closed and the whole system was stirred at room temperature for 48 h. The reaction

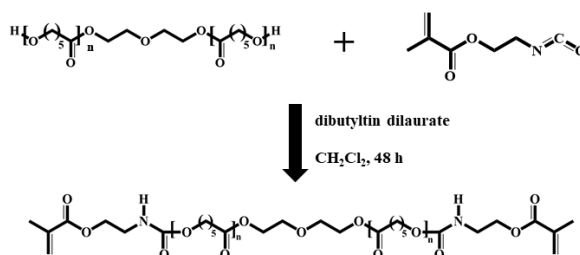
product was extracted and filtered from the solution by adding a large amount of petroleum ether, and then dried under vacuum at room temperature.



Scheme 2. Synthesis of POA-DA.

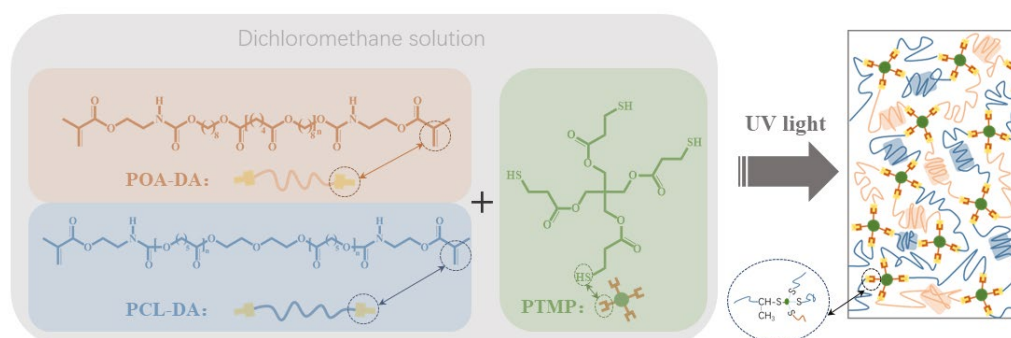
### 1.3 Synthesis of PCL-dimethacrylate (PCL-DA)

PCL-diol (5 g,  $0.5 \times 10^{-3}$  mol) was added to a single-mouth flask. Then, 25 mL of dichloromethane was added to the flask. After PCL-diol was completely dissolved, 2,2-isocyanatoethyl methacrylate (0.19 g,  $1.25 \times 10^{-3}$  mol) and dibutyltin dilaurate (0.1 mL) were added, where dibutyltin dilaurate served as a catalyst. Subsequently, the flask was closed and the whole system was stirred at room temperature for 48 h. The reaction product was extracted and filtered from the solution by adding a large amount of petroleum ether, and then dried under vacuum at room temperature.



Scheme 3. Synthesis of PCL-DA.

## 1.4 C-POA<sub>x</sub>PCL<sub>y</sub> polymer networks



Scheme 4. Synthesis of C-POA<sub>x</sub>PCL<sub>y</sub> polymer networks.

## 2. Characterization and test methods

### 2.1 Proton Nuclear Magnetic Resonance (<sup>1</sup>H NMR)

The structure in the chemical intermediates (including PCL-diol, POA-diol, POA-DA and PCL-DA) was determined by <sup>1</sup>H NMR in CDCl<sub>3</sub> solvent using a Bruker AVIII400 NMR spectrometer (400 MHz) at room temperature.

### 2.2 Test Methods for Determining Gel Content

The equilibrium swelling experiments were measured for all polymer networks (including C-POA, C-PCL and C-POA<sub>x</sub>PCL<sub>y</sub> polymer networks) to obtain the swelling degree and gel content of the corresponding networks. All samples were weighed (mass recorded as  $m_1$ ), and then placed into closed sample bottles containing large amounts of toluene. All samples were swelled at room temperature (23±2) °C. Each sample was removed and its surface was wiped at intervals of 24 h. Subsequently, the samples were weighed (mass recorded as  $m_2$ ). When the difference between the  $m_2$  values obtained twice consecutively was less than 0.002 g, swelling equilibrium was considered to have been reached. In addition, all swollen samples were removed and dried in vacuum at

80°C for 24 h. The dried samples were weighed (mass recorded as  $m_3$ ). The swelling degree (Q) and gel content (G) were calculated by the following equations:

$$Q = \frac{m_1/\rho_1 + (m_2 - m_1)/\rho_c}{m_1/\rho_1}$$

$$G = \frac{m_3}{m_1} \times 100\%$$

$\rho_1$  is the density of each sample before swelling.  $\rho_c$  is the density of toluene.

### 2.3 DSC analysis

The thermal properties of the C-POA, C-PCL and C-POA<sub>x</sub>PCL<sub>y</sub> polymer networks were measured with differential scanning calorimetry (METTLER-TOLEDO DSC 2). The melting temperature ( $T_m$ ) and the cold crystallization temperature ( $T_{cc}$ ) were obtained from the second heating scan and cooling scan, respectively.  $\Delta H_m$  is derived from the melting peak area on DSC curves in the second heating scan. The degree of crystallinity of the C-POA<sub>x</sub>PCL<sub>y</sub> polymer networks was calculated by the following equation:

$$\chi_c = \frac{\Delta H_m}{\Delta H_m^0[1] \cdot x + \Delta H_m^0[2] \cdot y}$$

Where  $\Delta H_m^0[1]$  is the enthalpy change of melting for a 100% crystalline C-POA, and the enthalpy values of 117.2 J•g<sup>-1</sup> is used<sup>1</sup>;  $\Delta H_m^0[2]$  is the enthalpy change of melting for a 100% crystalline C-PCL, and the enthalpy values of 135.0 J•g<sup>-1</sup> is used<sup>2</sup>. Moreover, x is the weight fraction of the POA segment content in the polymer sample, and y is the weight fraction of the PCL segment content in the polymer sample.

### 2.4 Fourier transform infrared spectroscopy (FTIR)

The FTIR in the POA-DA, PCL-DA, C-POA, C-PCL and C-POA<sub>x</sub>PCL<sub>y</sub> polymer networks) was recorded with Cary660+620 FT-IR micro infrared spectrometer (Agilent)

at room temperature.

## 2.5 Water absorption test

All samples were put into closed glass bottles containing deionized water. Then, they were stored in the dark at room temperature (about 20 °C). After 24 h, the weight of each sample was measured (the moisture on the sample surface was wiped). The water absorption ( $\omega_\alpha$ ) was calculated according to the following equation:

$$\omega_\alpha = \frac{m_2 - m_1}{m_1} \times 100\%$$

$m_1$  is the weight of the sample before immersion.  $m_2$  is the weight of the sample after it was immersed in water for 24 h.

## 2.6 Gel permeation chromatography (GPC)

The number average molecular weights ( $M_n$ ) and polydispersity index (PDI) of POA-diol and PCL-diol were measured on PL-GPC220 gel permeation chromatography (GPC) equipped with a PLgel 5 mm MIXED-D column with a dimension of 300×7.5 mm and a refractive index detector. HPLC grade chloroform was used as elution solvent at 40°C with a flow rate of 1.0 mL·min<sup>-1</sup>, and molecular weight was calibrated with polystyrene standard (3070-258 000 g·mol<sup>-1</sup>). The concentration of the sample was about 6.7 mg·mL<sup>-1</sup>.

## 2.7 X-ray diffraction (XRD)

X-ray diffraction (XRD) measurements of the synthesized C-POAxPCLy polymer networks were carried out using a D8 advance X-ray diffractometer (BRUKER, Germany). The CuK  $\alpha$  radiation ( $\lambda = 0.154$  nm) is used which is generated using an applied voltage of 20 kV. The spectra are registered in the 2-theta range of 5 to 60°

within 10 min.

## **2.8 The cytotoxicity test method**

The cytotoxicity assay was performed using the MTT method. The C-POA<sub>3</sub>PCL<sub>7</sub> sample was sterilized by UV irradiation for 30 min, and clipped into a 24-well plate. The suspension of HSAS1 cells was co-cultured with the material at 5% CO<sub>2</sub> and 37°C for 24 h. Subsequently, 500 uL of medium containing 0.5 mg/mL MTT was added to the system and incubated for 4 h. Then, the system was aspirated with medium and 600 μL of DMSO was added. The full wavelength enzyme standard (OD=570) was adopted for detection. The survival rate was calculated as follows: survival rate (100%) = OD of experimental group/OD of blank group\*100%.

## **3. Sample treatment**

### **3.1 Sample pretreatment before SAXS and WAXS tests**

The stretched C-POA<sub>3</sub>PCL<sub>7</sub> network in SAXS and WAXS analyses was obtained by Dynamic Thermal Mechanical (DMA) Analyzer. The spline sample (20 mm (length) × 5 mm (width) × 0.5 mm (thickness)) was heated to 65°C to eliminate thermal history and then was loaded 0.8 MPa stress immediately at axis of length. While keeping the stress unchanged, the temperature was reduced from 65°C to -30°C at 5 °C•min<sup>-1</sup>, and the temperature was kept at -30°C for a certain time. Afterward, the stress was unloaded, and the sample was removed from analyzer when the temperature returned to room temperature.

### **3.2 Preprogramming of samples required for complex reversible actuation**

The presentation examples' original temporary shape of [Fig. 2](#) and [Fig. 4](#) were

fabricated by manual pre-fixing before heat-treatment. Pre-fixing samples were heated to 80°C and then immediately immersed in liquid nitrogen for a few minutes. They were taken out, and the fixation was removed when they were restored to room temperature.

#### 4. Thermal Properties of C-PCL, C-POA and C-POA<sub>x</sub>PCL<sub>y</sub> polymer networks

Table S1. Thermal Properties of C-PCL, C-POA and C-POA<sub>x</sub>PCL<sub>y</sub> polymer networks.

| Sample                              | OA : CL<br>(wt% : wt%) | $T_m$ (°C) | $T_{cc}$ (°C) | $\Delta H_m$ (J/g) | $\chi_c$ (%) |
|-------------------------------------|------------------------|------------|---------------|--------------------|--------------|
| C-PCL                               | 0 : 1                  | 44.2       | 14.3          | 31.7               | 23.2         |
| C-POA <sub>1</sub> PCL <sub>9</sub> | 1 : 9                  | 41.0       | 5.9           | 32.4               | 24.1         |
| C-POA <sub>3</sub> PCL <sub>7</sub> | 3 : 7                  | 38.1       | 6.7           | 23.8               | 18.2         |
| C-POA <sub>4</sub> PCL <sub>6</sub> | 4 : 6                  | 38.7       | 9.5           | 29.5               | 22.8         |
| C-POA <sub>5</sub> PCL <sub>5</sub> | 5 : 5                  | 40.1       | 12.3          | 31.5               | 24.8         |
| C-POA <sub>6</sub> PCL <sub>4</sub> | 6 : 4                  | 43.1       | 18.3          | 37.5               | 30.1         |
| C-POA <sub>7</sub> PCL <sub>3</sub> | 7 : 3                  | 47.3       | 20.9          | 31.7               | 25.8         |
| C-POA <sub>9</sub> PCL <sub>1</sub> | 9 : 1                  | 48.1       | 25.6          | 34.7               | 28.6         |
| C-POA                               | 1 : 0                  | 52.7       | 31.0          | 49.1               | 41.9         |

## 5. Supplementary Figures

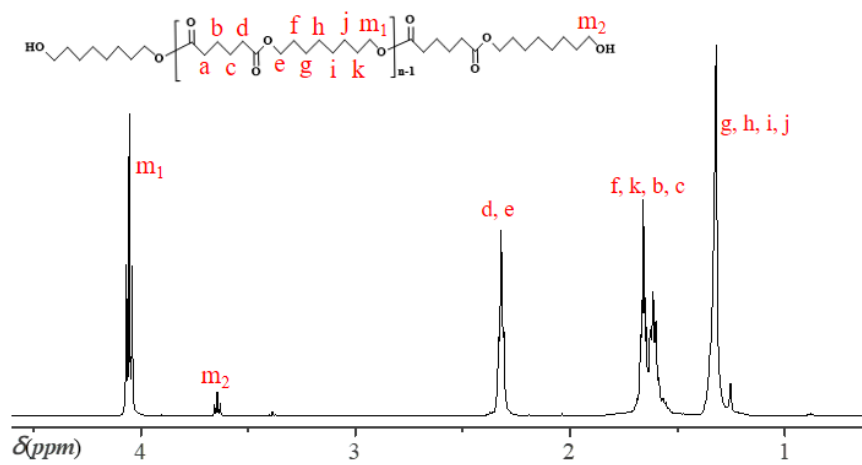


Fig. S1. <sup>1</sup>H NMR spectra (CDCl<sub>3</sub>, 400 MHz) of POA-diol.

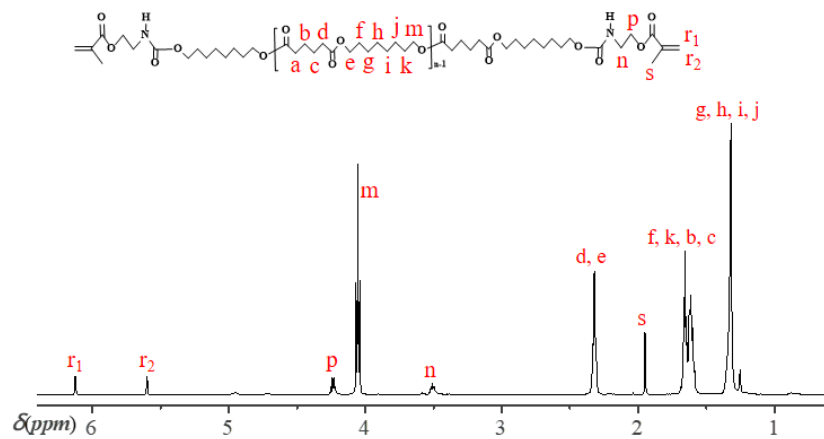


Fig. S2.  $^1\text{H}$  NMR spectra ( $\text{CDCl}_3$ , 400 MHz) of POA-DA.

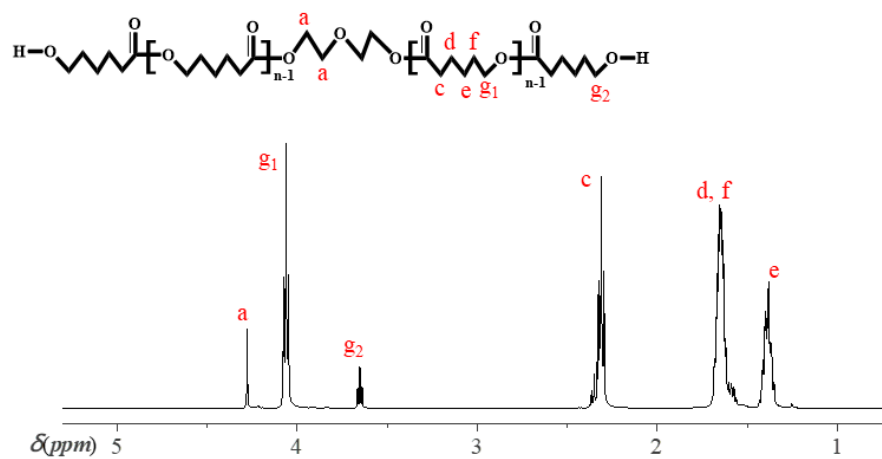


Fig. S3.  $^1\text{H}$  NMR spectra ( $\text{CDCl}_3$ , 400 MHz) of PCL-diol.

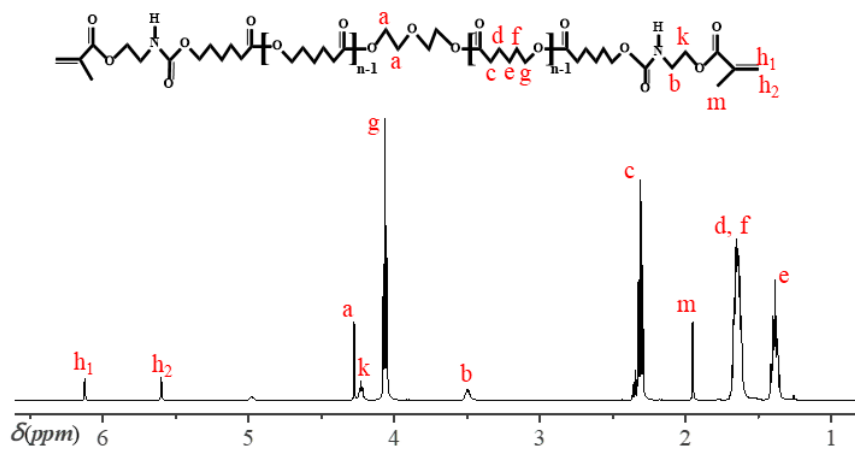


Fig. S4. <sup>1</sup>H NMR spectra (CDCl<sub>3</sub>, 400 MHz) of PCL-DA.

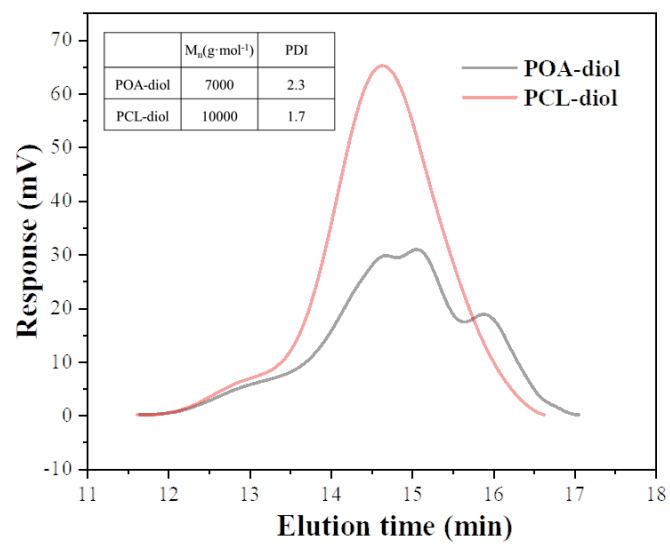


Fig. S5. The GPC curves of POA-diol and PCL-diol.

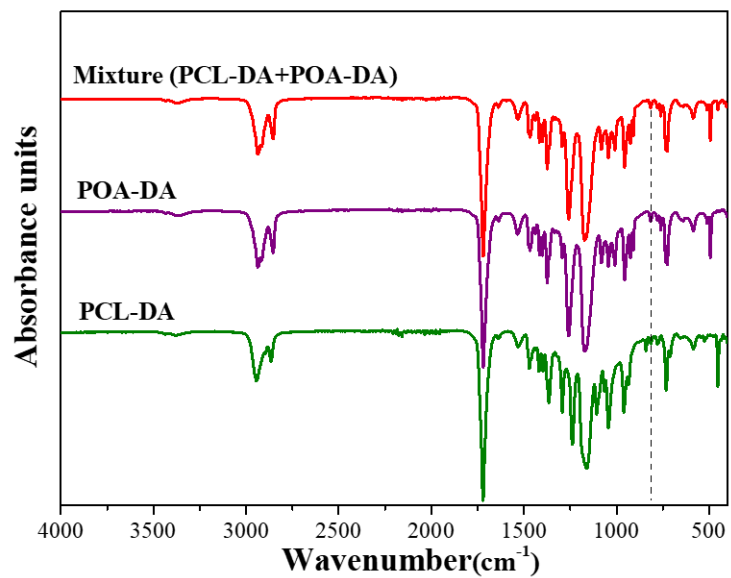


Fig. S6. FT-IR spectrum of POA-DA, PCL-DA and Mixture (PCL-DA+POA-DA).

The dotted line means the absorption intensity of the =CH at 811cm<sup>-1</sup>.

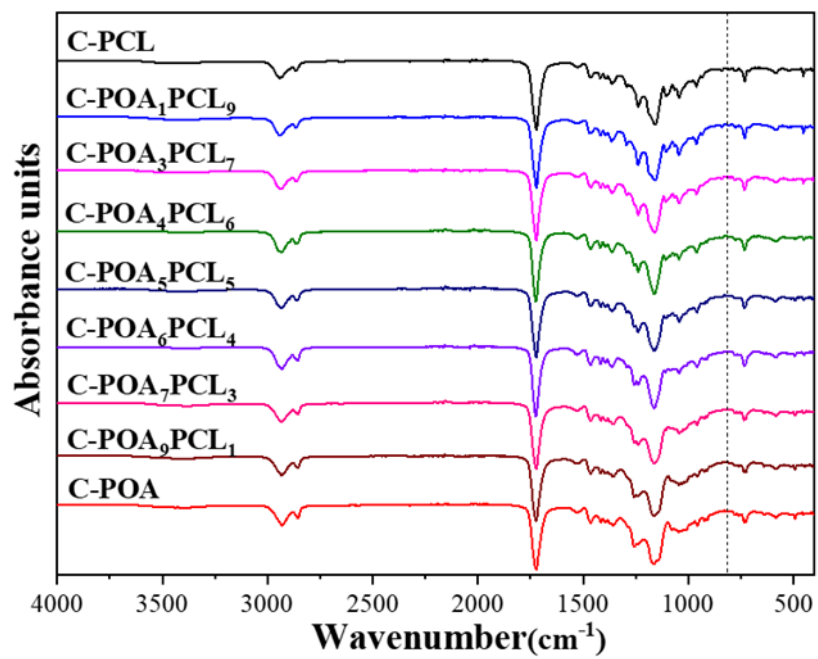


Fig. S7. FT-IR spectrum of C-PCL, C-POA and C-POA<sub>x</sub>PCL<sub>y</sub> polymer networks. The dotted line means the absorption intensity of the =CH at 811cm<sup>-1</sup>.

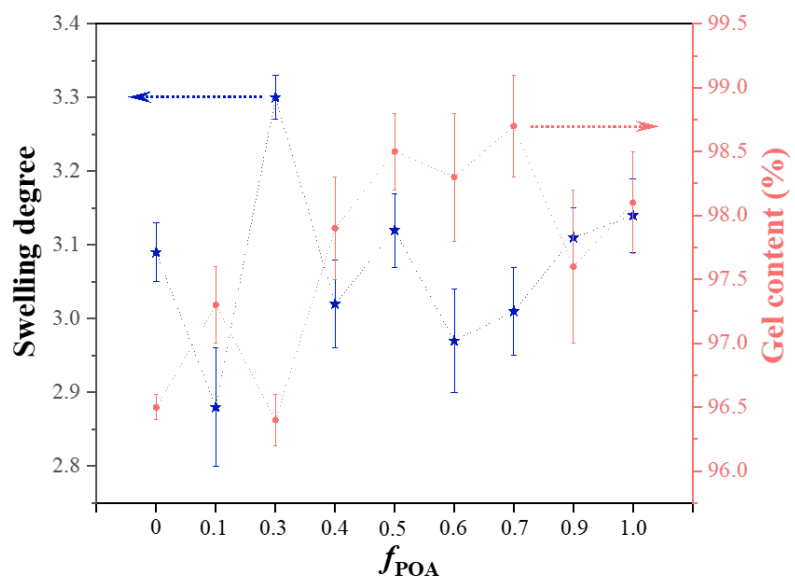


Fig. S8. Statistical distribution of the swelling degree and gel content of C-POA, C-PCL, and C-POA<sub>x</sub>PCL<sub>y</sub> polymer networks.

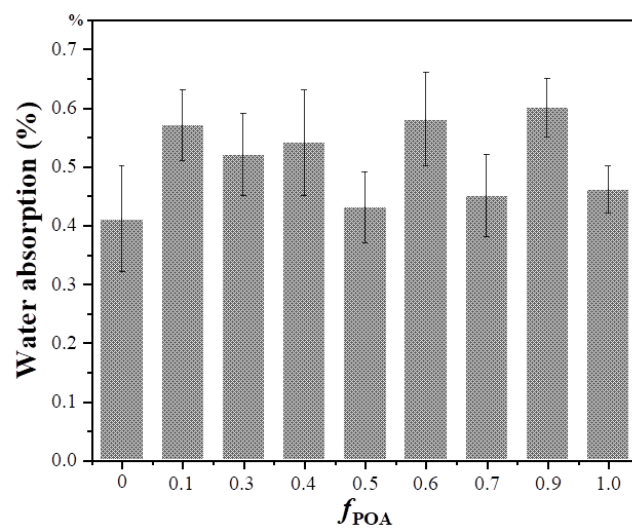


Fig. S9. The water absorption of the C-POA<sub>x</sub>PCL<sub>y</sub> polymer networks with change of

$f_{\text{POA}}$ .

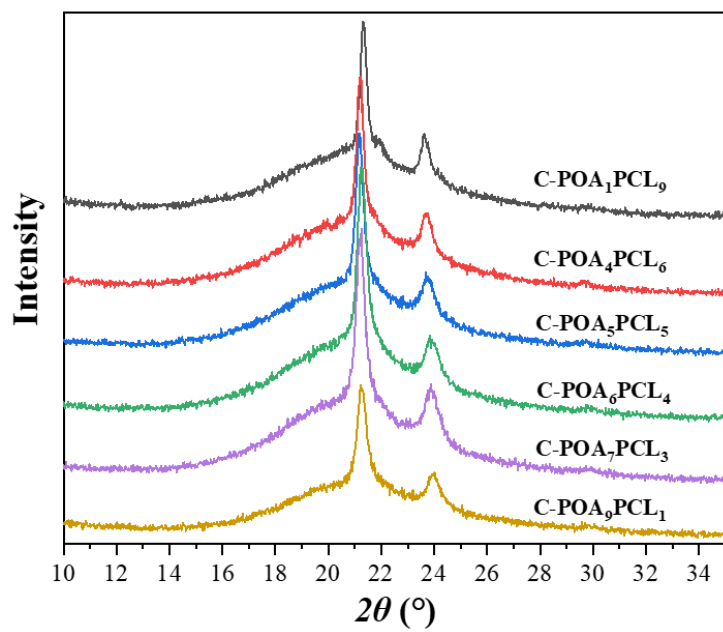


Fig. S10. WAXD curves of the C-POA<sub>x</sub>PCL<sub>y</sub> copolymer networks.

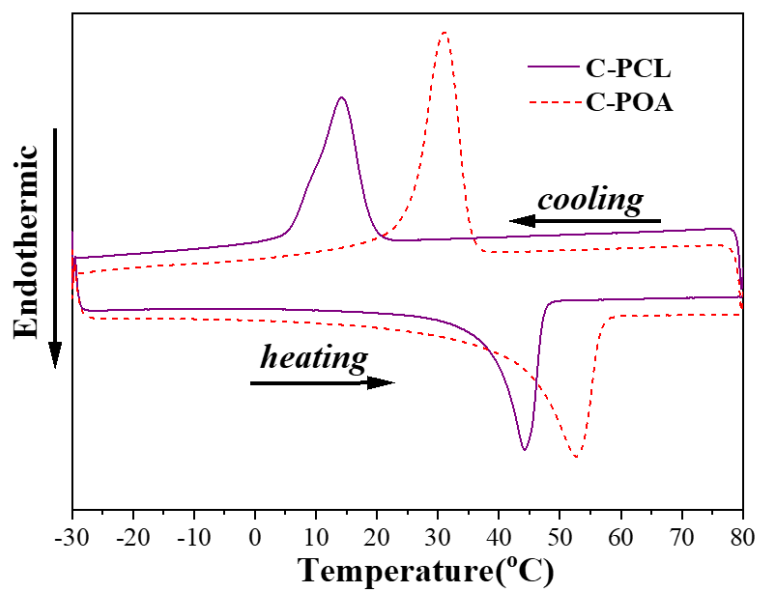


Fig. S11. DSC traces of C-POA (purple solid line) and C-PCL (red dotted line) in the second heating scans and cooling scans.

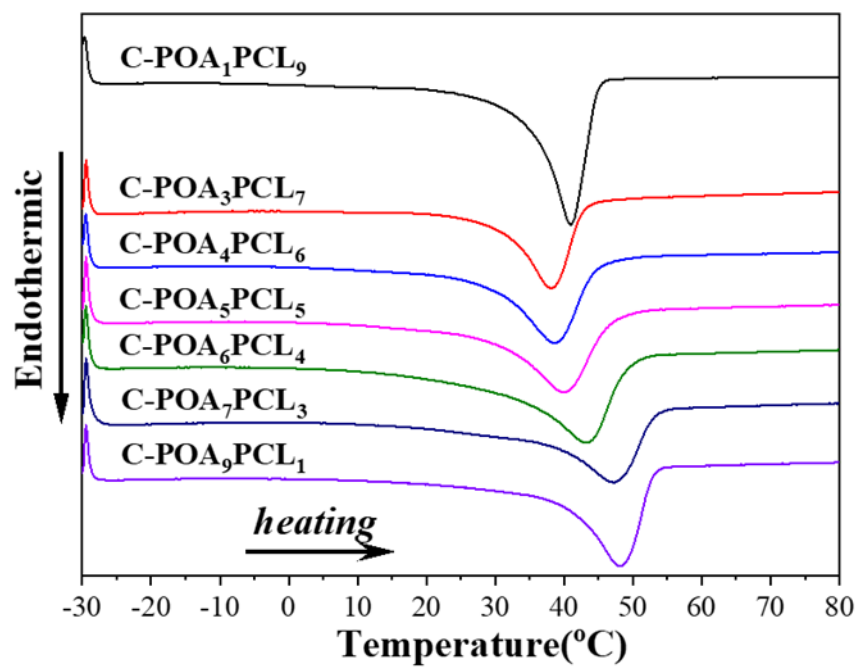


Fig. S12. DSC traces of C-POA<sub>x</sub>PCL<sub>y</sub> copolymer networks in the second heating scans.

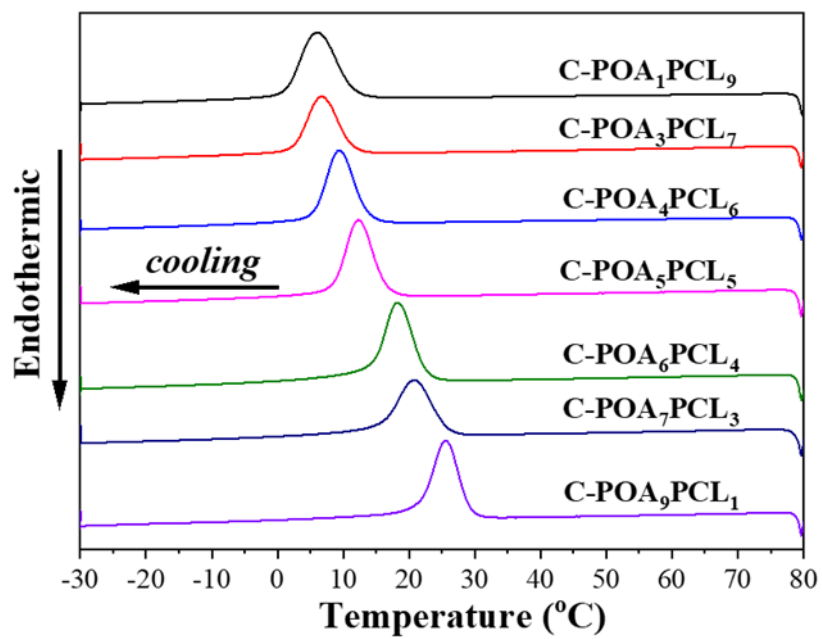


Fig. S13. DSC traces of C-POA<sub>x</sub>PCL<sub>y</sub> polymer networks in the cooling scans.

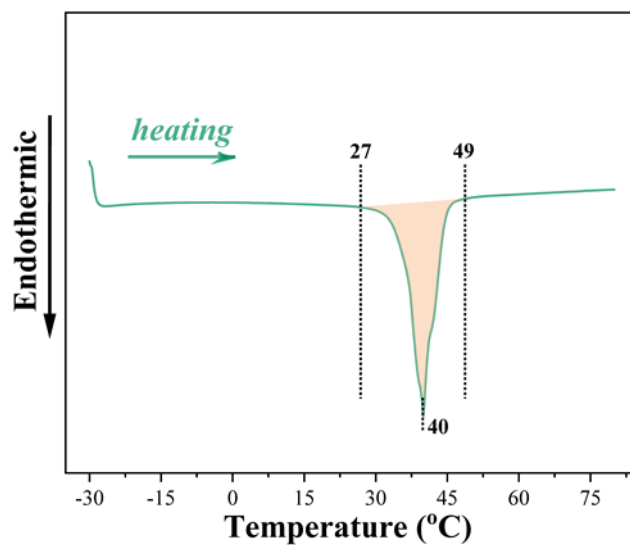


Fig. S14. DSC traces of C-POA<sub>3</sub>PCL<sub>7</sub> stretched sample in the first heating scans.

The stretched sample was obtained by firstly annealing at 80°C and then crystallizing at cooling when it was stretched to 100% strain.

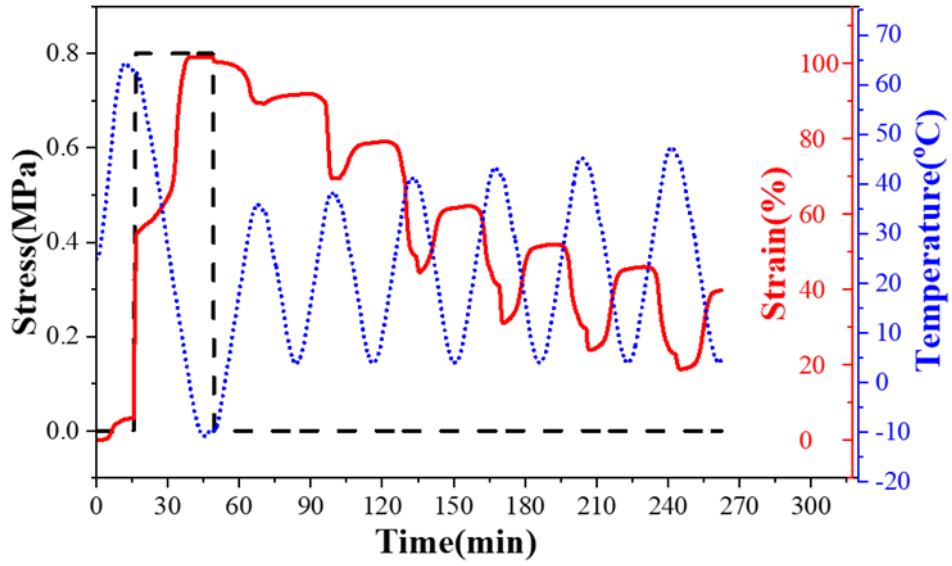


Fig. S15. Two-way shape memory cycles of the C-POA<sub>4</sub>PCL<sub>6</sub> polymer network between various  $T_{\text{high}}$  values and 4°C ( $T_{\text{low}}$ ). The corresponding  $T_{\text{high}}$  values were 36°C, 38°C, 41°C, 43°C, 45°C, and 47°C, respectively.

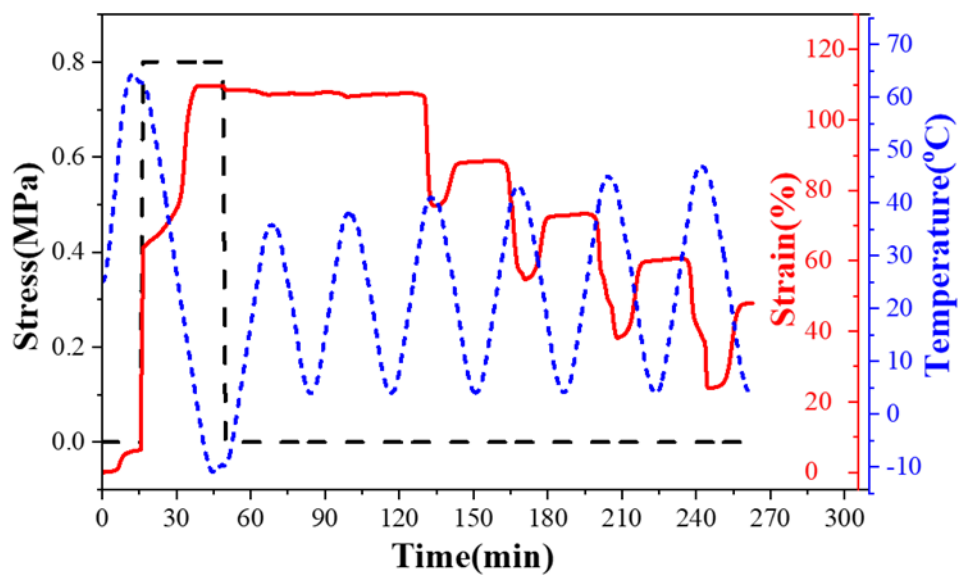


Fig. S16. Two-way shape memory cycles of the C-POA<sub>1</sub>PCL<sub>9</sub> polymer network between various  $T_{\text{high}}$  values and 4°C ( $T_{\text{low}}$ ). The corresponding  $T_{\text{high}}$  values were 36°C, 38°C, 41°C, 43°C, 45°C, and 47°C, respectively.

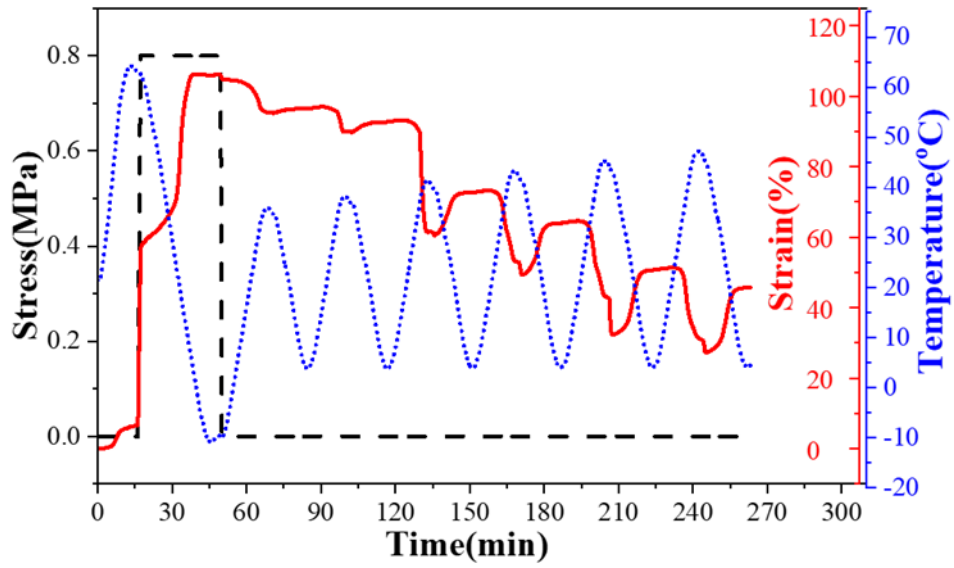


Fig. S17. Two-way shape memory cycles of the C-POA<sub>5</sub>PCL<sub>5</sub> polymer network between various  $T_{\text{high}}$  values and 4°C ( $T_{\text{low}}$ ). The corresponding  $T_{\text{high}}$  values were 36°C, 38°C, 41°C, 43°C, 45°C, and 47°C, respectively.

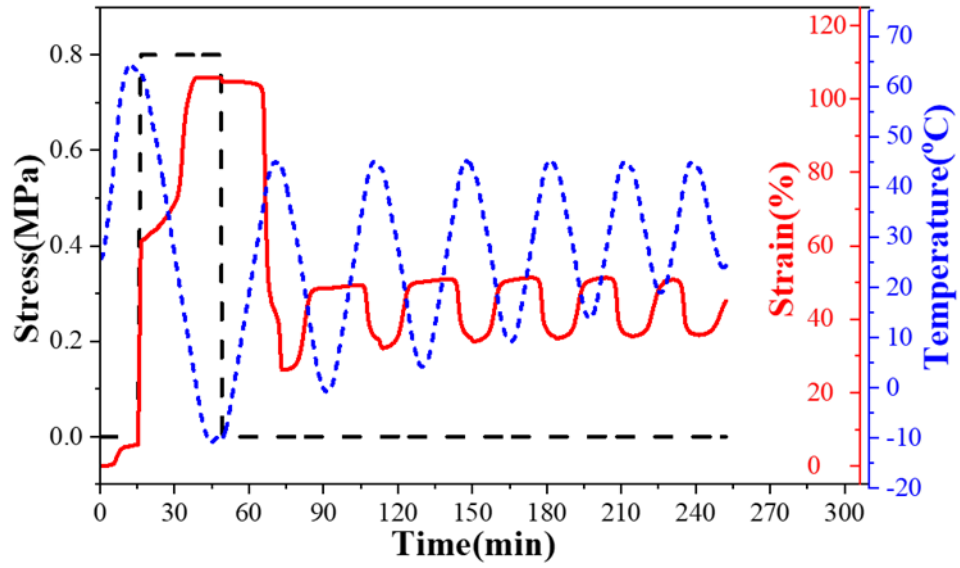


Fig. S18. Two-way shape memory cycles of the C-POA<sub>1</sub>PCL<sub>9</sub> polymer network between 45°C ( $T_{\text{high}}$ ) and various  $T_{\text{low}}$  values. The corresponding  $T_{\text{low}}$  values were 0°C, 4°C, 9°C, 14°C, 19°C and 24°C, respectively.

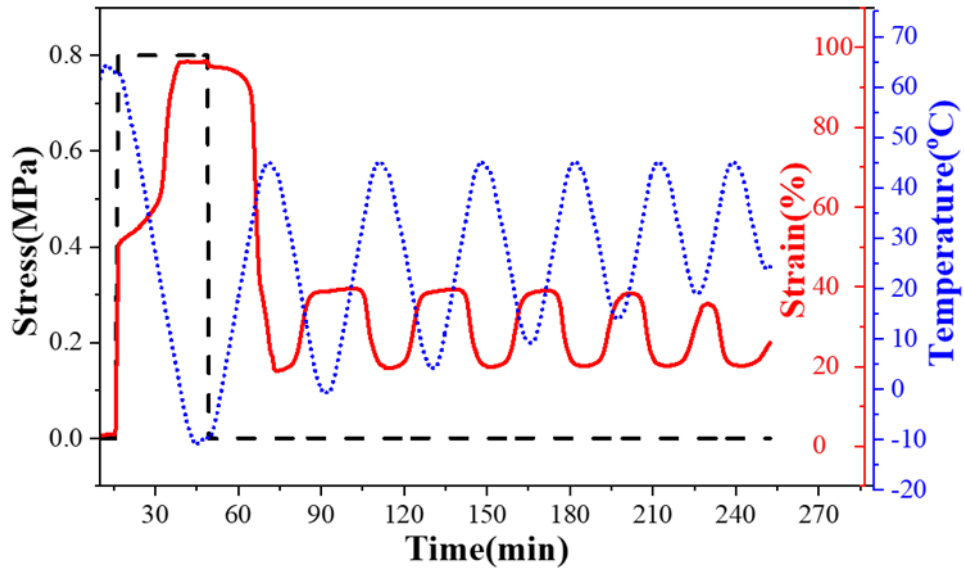


Fig. S19. Two-way shape memory cycles of the C-POA<sub>4</sub>PCL<sub>6</sub> polymer network between 45°C ( $T_{\text{high}}$ ) and various  $T_{\text{low}}$  values. The corresponding  $T_{\text{low}}$  values were 0°C, 4°C, 9°C, 14°C, 19°C and 24°C, respectively.

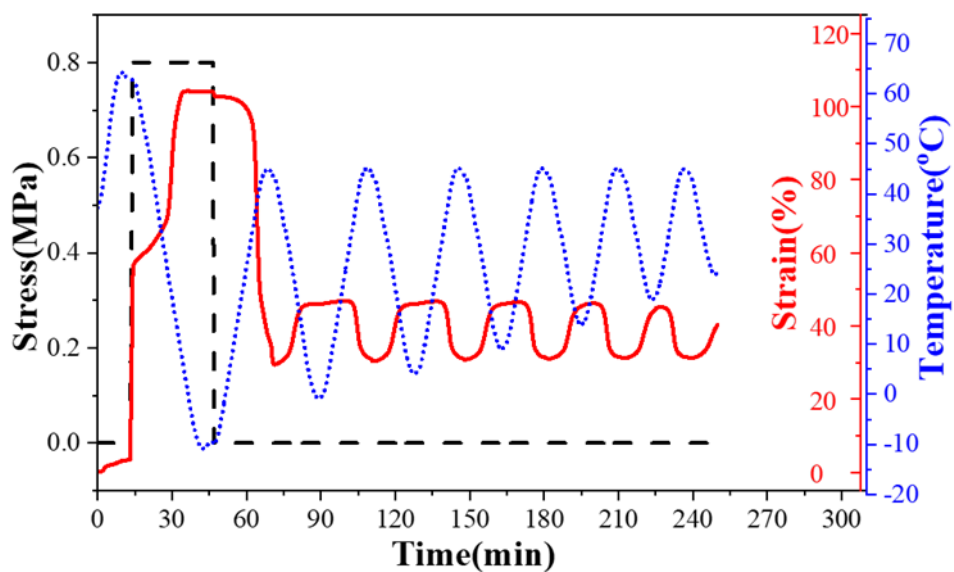


Fig. S20. Two-way shape memory cycles of the C-POA<sub>5</sub>PCL<sub>5</sub> polymer network between 45°C ( $T_{\text{high}}$ ) and various  $T_{\text{low}}$  values. The corresponding  $T_{\text{low}}$  values were 0°C, 4°C, 9°C, 14°C, 19°C and 24°C, respectively.

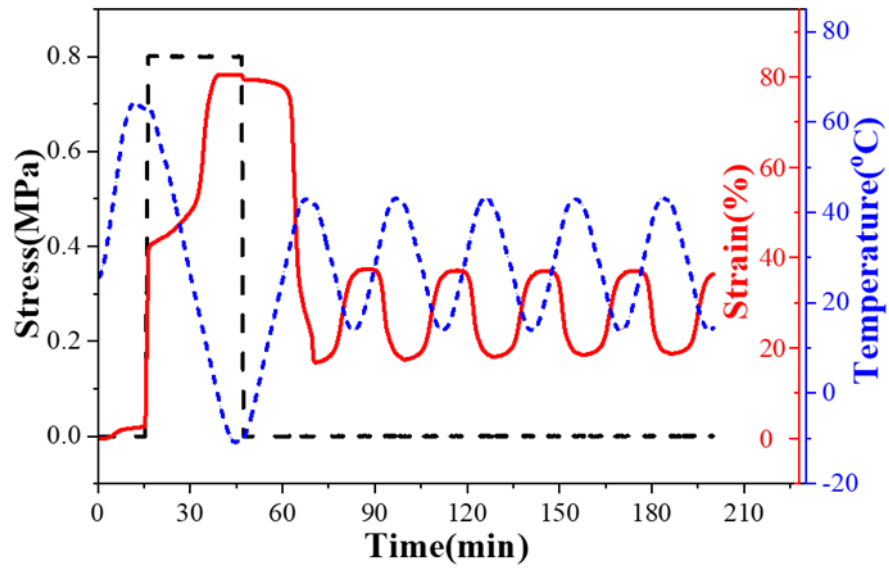


Fig. S21. Stable 2W-SME cycles of C-POA<sub>3</sub>PCL<sub>7</sub> network between  $T_{\text{high}}=43^{\circ}\text{C}$  and  $T_{\text{low}}=14^{\circ}\text{C}$ .

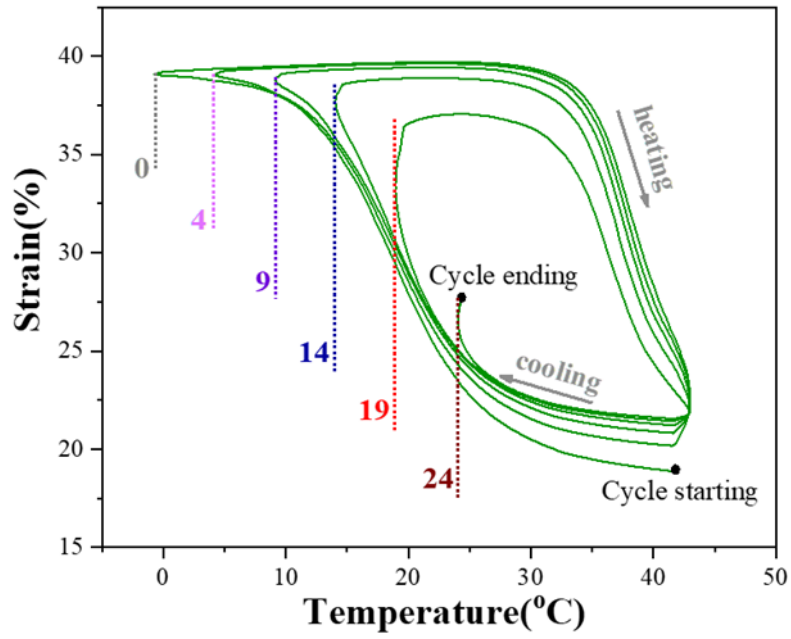


Fig. S22. Strain curves of the C-POA<sub>3</sub>PCL<sub>7</sub> network that were reversibly actuated between a variable  $T_{low}$  value ranging from 0°C to 24°C and a fixed  $T_{high}$  value of 43°C.

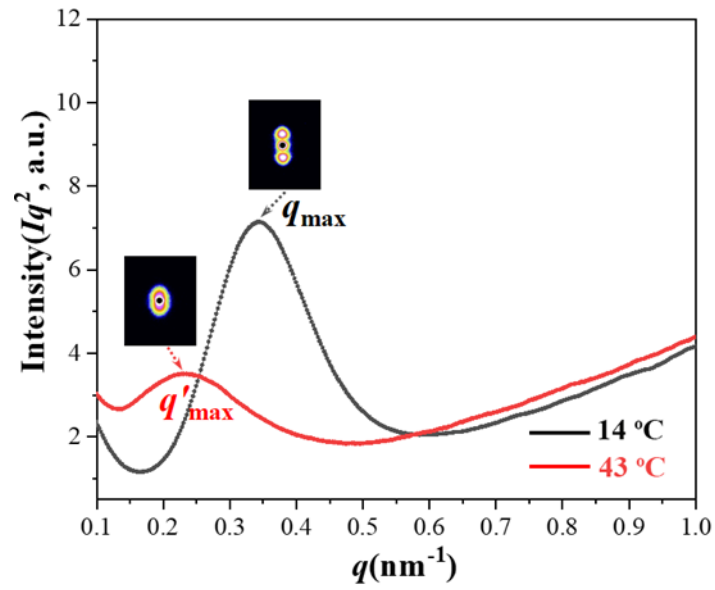


Fig. S23. One-dimensional small-angle X-ray scattering (SAXS) curves changes occurring during the 2W-SME of C-POA<sub>3</sub>PCL<sub>7</sub> polymer network in subsequent reversibility cycles at between  $T_{\text{high}} = 43^\circ\text{C}$  and  $T_{\text{low}} = 14^\circ\text{C}$ .

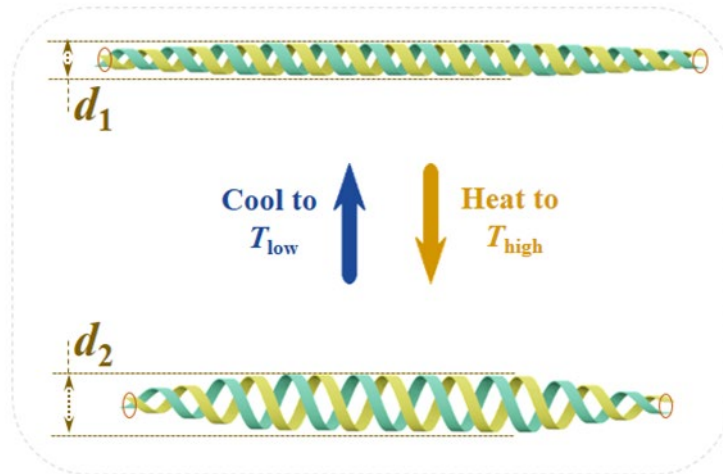


Fig. S24. Graphic illustration of the change of double-helix structure in 2W-SME. The color of the spiral structure is only used to identify it as a double-helix rather than a single-helix, and has no other special meaning.  $d_1$  and  $d_2$  represent the diameter of the spiral structure.

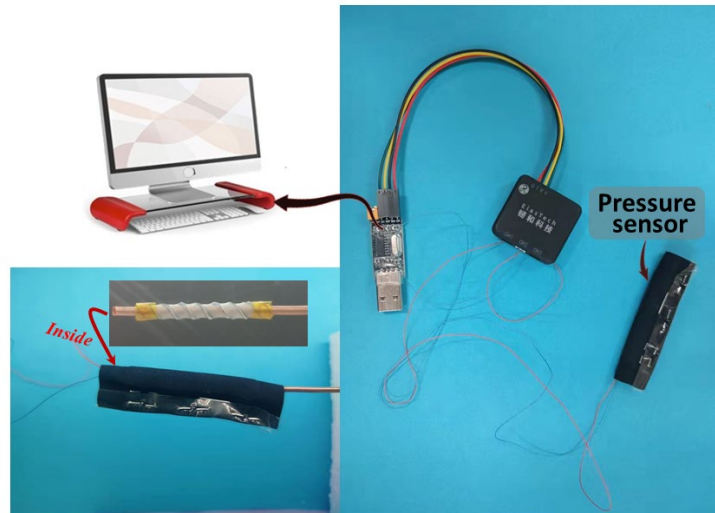


Fig. S25. A flexible mechanical sensor that could detect the pressure on the inner wall of the sensor when the spiral structure expands in real time.

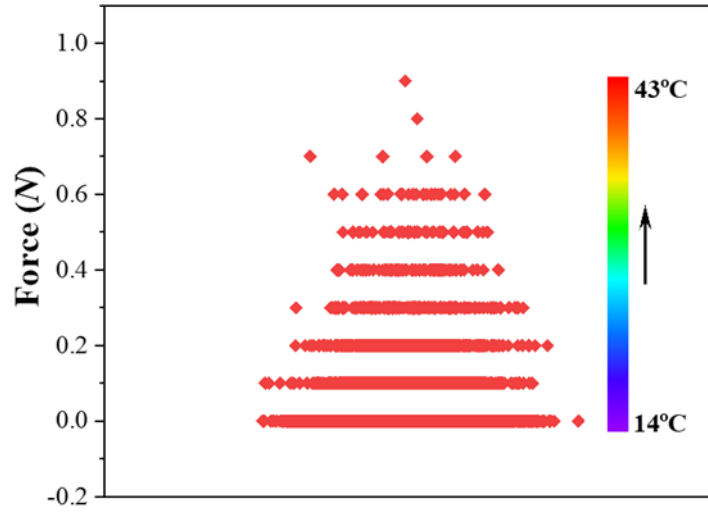


Fig. S26. The relationship between the pressure and temperature on the sensor.

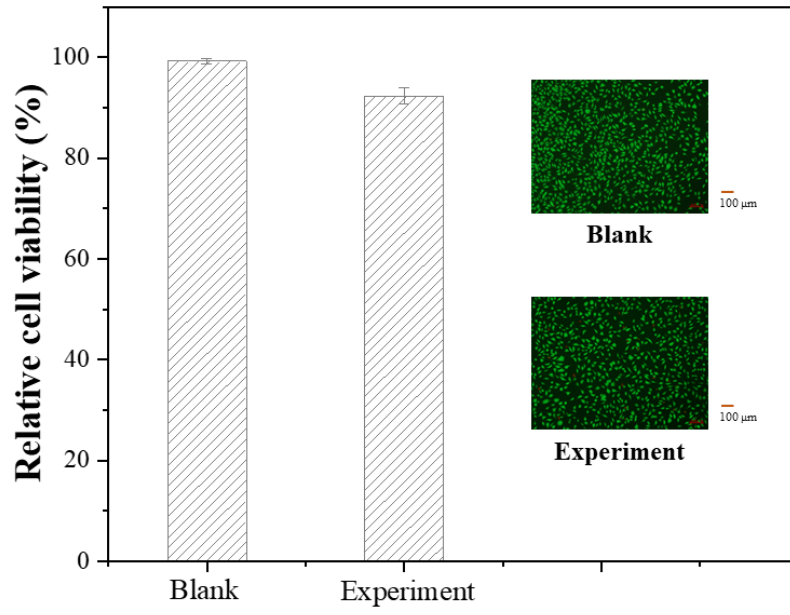


Fig. S27. Effect of the C-POA<sub>3</sub>PCL<sub>7</sub> network on the relative viability of cells.

## 6. Supplementary Videos

**Video S1.** Shape change between closing and unfolding of 3D-tubular curl of C-POA<sub>3</sub>PCL<sub>7</sub> network through heating to  $T_{\text{high}}$  of 43°C and cooling to  $T_{\text{low}}$  of 14°C.

**Video S2.** Cooperative shape change of 3D-support structure in space via paper-cutting art between 43°C and 14°C.

**Video S3.** A soft gripper was designed through customized paper-cutting art. The gripper closed and opened during cooling–heating cycles, respectively, and was used to move a small box with a handle.

**Video S4.** The rotating expansion and contraction process of double-helix structure to complete the drug release and vehicle recovery progress based on the 2W-SME of C-POA<sub>3</sub>PCL<sub>7</sub> network.

## 7. Supplementary References

1. X. Li and Z. Qiu, *Macromol. Res.*, 2015, **23**, 678-685.
2. W. Yuan, K. Liu, J. Zhou, L. Ni, G. Shan, Y. Bao and P. Pan, *ACS Macro Lett.*, 2020, **9**, 1325-1331.